Geometrical barriers and lower critical field in MgB2 single crystals

L. Lyard, Thierry Klein, J. Marcus, R. Brusetti, C. Marcenat, M. Konczykowski, V. Mosser, K.H. Kim, B.W. Kang, H.S. Lee, et al.

PHYSICAL REVIEW B **70**, 180504(R) (2004)

Geometrical barriers and lower critical field in MgB_2 single crystals

L. Lyard,[1] T. Klein,[1,2] J. Marcus,[1] R. Brusetti,[3] C. Marcenat,[4] M. Konczykowski,[5] V. Mosser,[6] K. H. Kim,[7] B. W. Kang,[7] H. S. Lee,[7] and S. I. Lee[7]

[1]*Laboratoire d'Etudes des Propriétés Electroniques des Solides, CNRS, Boîte Postale 166, 38042 Grenoble Cedex 9, France*

[2]*Institut Universitaire de France and Université Joseph Fourier, Boîte Postale 53, 38041 Grenoble Cedex 9, France*

[3]*Centre de Recherche sur les Très Basses Températures, Centre National de la Recherche Scientifique, Boîte Postale 166, 38042 Grenoble Cedex 9, France*

[4]*Département de Recherche Fondamentale sur la Matière Condensée, Commissariat à l'Energie Atomique - Grenoble, SPSMS, 17 Rue des Martyrs, 38054 Grenoble Cedex 9, France*

[5]*Laboratoire des Solides Irradiés, Ecole Polytechnique, 91128 Palaiseau, France*

[6]*Schlumberger Utilities Technology Group, 50 avenue Jean Jaures, Boîte Postale 620-13, F-92542 Montrouge, France*

[7]*NVCRICS and Department of Physics, Pohang University of Science and Technology, Pohang 790-784, Republic of Korea*

(Received 6 August 2004; published 30 November 2004)

The first penetration field (H_p) has been deduced from local magnetization and specific heat measurements in magnesium diboride single crystals. For $H_a^{\parallel c}$, the geometrical barriers (GB) play a dominant role in the irreversibility mechanism. In thin samples, neglecting the GB in this direction would then lead to a large overestimation of H_{c1} deduced from H_p through the standard elliptical formula. The lower critical field is found to be isotropic at low temperature ($\sim 0.11 \pm 0.01$ T).

DOI: 10.1103/PhysRevB.70.180504 PACS number(s): 74.25.Op, 74.25.Qt

MgB_2 is the first example of a superconductor ($T_c \sim 39$ K)[1] presenting two distinct superconducting gaps.[2] Indeed, it is now well established that MgB_2 is characterized by a complex Fermi surface showing two sections: a three-dimensional (3D) tubular network of mostly boron π states and two-dimensional (2D) cylindrical sheets derived mostly from boron σ states. The coexistence of those two gaps with different anisotropies leads to an *anomalous decrease* of the anisotropy of the upper critical field (H_{c2}) with temperature.[3,4] On the contrary, we have recently shown[5] that the anisotropy of the lower critical field (H_{c1}) *increases* by about 50% between 5 K and T_c. Nevertheless, the absolute values of $H_{c1}^c(0)$ (parallel to the c axis of the crystal) and $H_{c1}^{ab}(0)$ (in the basal plane) still had to be to determined accurately. $\Gamma_{H_{c1}}(0) = H_{c1}^c / H_{c1}^{ab}$ is a very important parameter in the two-band superconductor scenario, which has been predicted to be close to 1 at low T.[6] However, previous measurements on single crystals led to $H_{c1}^c(0)$ values ranging from 0.05 (Ref. 7) [with $\Gamma_{H_{c1}}(0) \sim 1$] to 0.25 T [with $\Gamma_{H_{c1}}(0) \sim 2$].[8]

In samples with elliptical cross sections, H_{c1} can be deduced from the first penetration field H_p, assuming that the magnetization $M = -H_{c1}$ when the first vortex enters into the sample. As $M = -H_a/(1-N)$ in the Meissner state (where N is the demagnetization coefficient and H_a the external field), H_{c1} is thus related to H_p through

$$H_{c1} = \frac{H_p}{1-N}. \tag{1}$$

In "real" samples, i.e., with arbitrary cross sections, the M-H curve can still be approximated by a linear variation in the Meissner state and Eq. (1) is often still used to deduce H_{c1} from H_p in type II superconductors (replacing N by an effective demagnetization coefficient N_{eff}). However, considering only those "elliptical" demagnetizing effects can lead to an overestimation of H_{c1} due to the presence of surface [i.e., Bean-Livingston (BLB)][9] and/or geometrical barriers (GB).[10,11] GB are particularly important in thin samples as this overestimation is expected to vary as $\sqrt{w/d}$ (Refs. 10 and 11) (where $2w$ is the width of the sample). Indeed, in samples with rectangular cross sections, flux lines first penetrate into the sample through the sharp corners, leading to a position (x) dependent vortex energy per unit length reaching a maximum for $|x| \sim w - d/2$ (x being equal to zero at the center of the sample).[10] The resulting barrier decreases with applied field but delays the vortex penetration (as compared to samples with elliptical cross sections); the magnetization at $H = H_p$ is larger than H_{c1} and the elliptical equation [Eq. (1)] is thus not valid anymore.

It has, for instance, been shown by Zeldov *et al.*[12] that GB play an important role in BiSrCaCuO crystals. To measure realibly the absolute value of H_{c1} in MgB_2, it is thus necessary to determinine the origin of irreversibility in this system. We used a Hall probe array to get the field distribution in the samples, and we clearly show that, for low external fields $H_a \| c$, GB play a dominant role in the irreversibility mechanism of this system, too. Taking properly into account GB we deduced $H_{c1}^c(0) \sim 0.11 \pm 0.01$ T. Those effects can be neglected for $H \| ab$, and we obtained a very similar H_{c1}^{ab} value in this latter direction, confirming that $\Gamma_{H_{c1}} \sim 1$ at low temperature.[5,7]

We performed both magnetic and specific heat measurements in high-quality MgB_2 single crystals[13] showing flat surfaces. Nine samples with different lengths (l), widths ($2w$), and thicknesses (d) have been measured (see Table I). In samples 5–9 (see Table I), magnetic field profiles have been determined using a two-dimensional electron-gas (2DEG) Hall-probe array constituted of 11 inline sensors of 8×8 μm^2 active area and 20 μm separation (in samples 1–4

TABLE I. d, $2w$, and l are the thickness, width, and length of the samples, respectively. The first penetration field H_p has been defined as the field above which the local induction in the center of the sample becomes finite. The critical temperature T_c has been deduced from the onset of the diamagnetic response in ac susceptibility measurements.

Sample	d (μm)	$2w$ (μm)	l (μm)	H_p (G)	T_c (K)
1	10	200	250	150	36.4
2	2	13	19	270	34.4
3	5	30	40	350	34.4
4	50	230	250	380	37.5
5	40	140	230	420	36.2
6	30	90	230	370	36.2
7	70	200	470	400	36.2
8	20	50	120	410	35.1
9	50	100	170	450	36.2

we only measured the induction in the center of the sample as a function of H_a). Figure 1(a) shows a typical example of the profiles measured at low temperature (4.2 K) in sample 6. Each profile was obtained in a few seconds, and we checked that they were not time dependent by repeating the measurements several times. Complementary information was provided by specific heat (C_p) measurements (sample 4). Indeed, C_p is proportional to the number of vortices in the sample, and H_p can be detected by a rapid increase of C_p for $H > H_p$ (see Fig. 2). Note that this determination is independent on the distribution of the vortices (i.e., of the nature of pinning). C_p was measured by an ac technique[14] allowing us to measure small samples with high sensitivity (typically one part in 10^4). Heat was supplied to the sample by a light-emitting diode via an optical fiber, and the temperature oscillations were measured by a chromel-constantan thermocouple.

For applied fields $\mu_0 H_a < \mu_0 H_p$ ($\sim$0.037 T in sample 6), the external field is screened out, and $B \sim 0$ T for sensors 4–7 (see Fig. 3 for B vs H_a). For $H_a > H_p$, a maximum induction $B(x)$ is observed in the center of the sample (near sensor 6, i.e., for $x/w = 0$) and the field profiles are dome shaped (see Fig. 1). For bulk pinning (i.e., the Bean model[15]), a minimum should be observed in the center of the sample for ascending fields as vortices would remain pinned near surfaces by bulk defects. Such a unique accumulation of vortices in the center of the sample is typical of BLB and/or GB, reflecting the fact that, in the absence of bulk pinning, vortices are free to reach the center of the sample for $H > H_p$. The importance of those barriers is further confirmed by plotting the field gradient dB/dx on ascending and descending branches of the loop [see Fig. 1(b)]. In the case of bulk pinning, according to the Bean model, dB/dx is proportional to the critical current, and the field gradient on ascending field dB/dx_{up} is opposite to the field gradient on descending field dB/dx_{down}: $dB/dx_{up} = -dB/dx_{down}$ (<0 for $x<0$). In contrast, BLB and GB lead to a positive dB/dx for $x<0$ for both increasing and decreasing fields with $dB/dx_{up} > dB/dx_{down} > 0$,[12] in good agreement with experimental data for $B \geqslant 0.05$ T [see Fig. 1(b)].

The difference between dB/dx_{up} and dB/dx_{down} becomes negligible above $\sim$0.15 T. In the presence of pure GB, the irreversible shielding is expected to vanish at $\approx 1.5\sqrt{w/d}\mu_0 H_p \sim 2\mu_0 H_p \sim 0.1$ T,[12] which is consistent with our experimental value $\sim$0.15 T. Similarly, the irreversibility should vanish for $B \to 0$. We did not observe this effect, clearly showing that a small amount of bulk pinning is also present in our samples. Indeed, as shown in Fig. 1(b), the field gradient dB/dx increases when the applied field tends towards zero and the field profiles present the typical pyramidal Bean model shape for low decreasing fields [see Fig. 1(a) at 0.01 T]. In the absence of bulk pinning, the field at the center of the sample B_0 is expected to vary as $B_0 \approx \mu_0 H_a \sqrt{1-(H_p/H_a)^2}$ for $H_a > H_p$ (Ref. 10) (see the solid line in Fig. 3 with $\mu_0 H_p = 0.037$ T). As shown, the experimental data lie slightly below the theoretical curve due to the presence of a small amount of bulk pinning ($\lesssim 5\times 10^4$ A/cm^2, in good agreement with our previous estimations of J_c from ac transmittivity measurements above 0.1 T).[3]

The first penetration field H_p has been deduced using four different criteria. (i) First, H_p has been directly deduced from the field profiles as being the field for which a finite B value could be measured in the sample (see Fig. 3). As bulk pin-

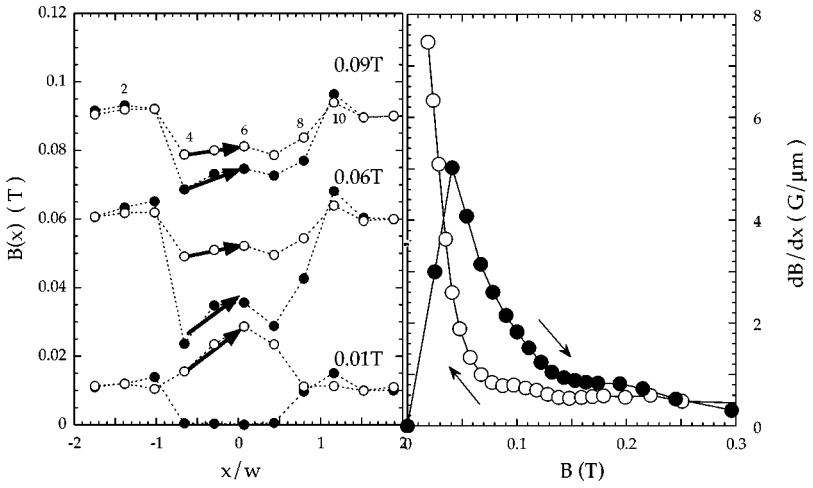

FIG. 1. (a) Magnetic field profiles for increasing (solid symbols) and decreasing (after having applied a maximum field of 1 T, open symbols) magnetic field in sample 6 (see Table I) at $T = 4.2$ K. (b) The magnetic field gradient as a function of the magnetic induction [probe 5, see arrows in Fig. 1(a)] clearly showing that the slope is larger for increasing fields than for decreasing ones as expected in the presence of Bean-Livingstone and/or geometrical barriers.

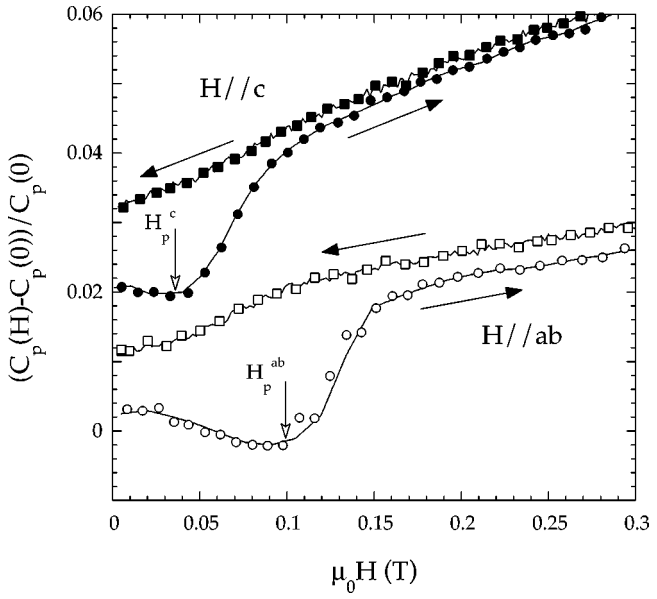

FIG. 2. Magnetic field dependence of the specific heat at $T \sim 6$ K for H parallel to the c axis (top) and ab plane (bottom). The data along the c axis have been shifted upwards for clarity. Within the calibration errors of the thermocouple, the specific heat is constant up to H_p and rapidly increases for higher magnetic fields. Vortices remain pinned in the sample for decreasing fields and C_p is clearly irreversible at low field.

ning is very small, this value is independent on the position of the probe, as shown in the inset of Fig. 3. (ii) We previously deduced H_p from the sharp minimum in the M_{av} vs H curve, where M_{av} is the average between the ascending and

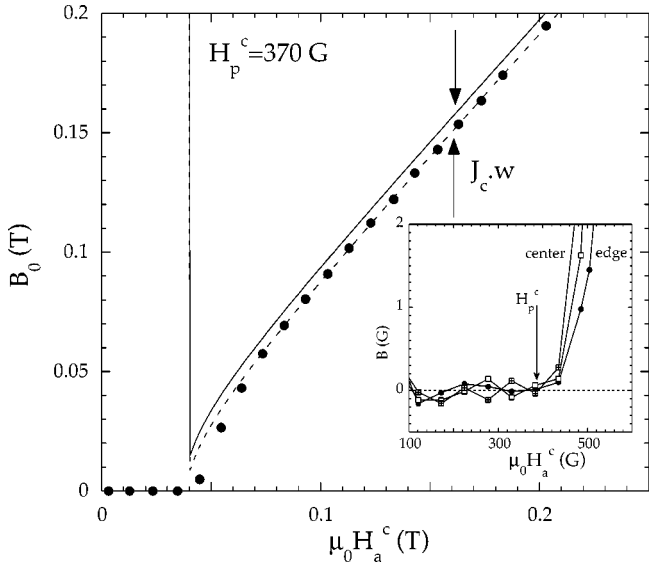

FIG. 3. Local induction at the center of the sample as a function of the external field (sample 5, $T=4.2$ K). The solid line is the dependence expected for pure geometrical barriers pinning. A small shift is observed (dotted line) due to the presence of a small amount of residual bulk pinning. Inset: local induction as a function of the external field for three probes from the edge to the center of the sample showing that H_p is independent on the probe position.

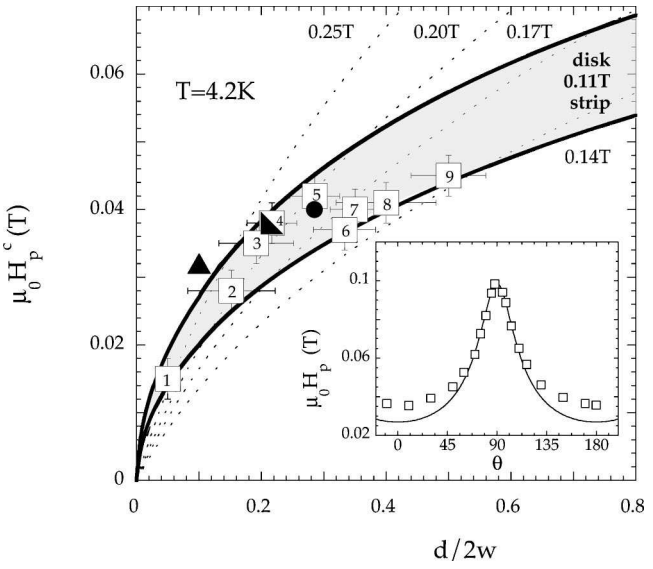

FIG. 4. First penetration field vs $d/2w$ for the different samples (see Table I). The solid lines are the dependences expected for disks and rectangular strips in the presence of GB taking $H_{c1}=0.11$ T. The filled circle is the H_p value previously deduced in Ref. 5 and the filled triangle is the one obtained by Ref. 8. For sample 4 (open/filled squares), both magnetic and specific heat measurements led to the same value. The dotted lines show the behaviors for strips with elliptical cross sections in which no geometrical pinning would be present. Inset: H_p as a function of the angle θ between the external field and the c axis. The solid line is a fit to the data using Eq. (3), i.e., assuming that no GB is present. As shown, the penetration is clearly delayed in the vicinity of the c axis due to the presence of those barriers.

descending branches of the local magnetization loop.[5] Even though this average does not exactly reproduce the reversible part of the magnetization in presence of GB (and/or BLB), we obtained the same H_p values using procedures (i) and (ii) (see the filled circle in Fig. 4). (iii) In this third procedure the remanent field in the sample has been measured after applying successively larger magnetic field cycles. A finite remanent field was then obtained for field amplitudes larger than H_p (due to the presence of some bulk pinning), and this procedure again led to the same H_p values in our samples. (iv) H_p was finally deduced from specific heat (C_p) measurements. Sample 4 has been cooled in zero magnetic field down to ~ 6 K. As shown in Fig. 2, C_p remains almost constant at low field (within the uncertainties of the thermocouple calibration) and sharply increases as vortices enter in the sample for $H > H_p$ (see Fig. 2, sample 3). We hence get $\mu_0 H_p^c \sim 0.038$ T and $\mu_0 H_p^{ab} \sim 0.1$ T, in excellent agreement with the values deduced from the magnetic measurements [procedure (i)]. Note that the anomaly at H_p is smeared out by the presence of residual bulk pinning in the descending branch of the curve. Some vortices remain pinned for $H < H_p$, leading to very different behaviors for the ascending and descending branches at low field.

The corresponding H_p values have been reported in Fig. 4 (open squares), together with the value previously estimated in Ref. 5 (filled circle) as well as the value obtained in Ref. 8 (filled triangle). Following Ref. 11, in the presence of geo-

metrical barriers, H_p is related to H_{c1} through

$$H_{c1} \approx \frac{H_p}{\tanh(\sqrt{\alpha d/2w})}, \quad (2)$$

where α varies from 0.36 in strips to 0.67 in disks. As shown, this behavior is consistent with our experimental data, taking $\mu_0 H_{c1} \sim 0.11 \pm 0.01$ T. Note that for samples 3 and 4, $l \sim 2w$, and those samples can be better described by the disk formula. The dotted lines in Fig. 4 have been deduced from Eq. (1) (i.e., neglecting GB) for strips with rectangular cross sections taking the N_{eff} values computed in Ref. 16. As shown, in this case, it would be impossible to describe our samples by a unique H_{c1} value. Neglecting GB would thus lead to an overestimation of H_{c1} ranging from 0.14 T (sample 9) up to 0.25 T (sample 3). Note that Eq. (2) is characteristic of GB, clearly showing that those barriers dominate in the irreversibility process for low applied fields. Indeed, in presence of BLB, the dependence of H_p on the sample geometry is expected to be again given by the $(1-N_{eff})$ factor but replacing H_{c1} by the thermodynamic field H_c.[18]

In a previous article,[5] we discussed the T dependence of the anisotropy of H_{c1} (and of H_{c2}) in which we gave a rough estimate of $H_{c1}^c(0)$ since we did not measure at that time the importance of GB. This estimate (0.10 T) happens to be close to the precise determination (0.11 T) found here, mainly due to the fact that this sample was "not too thin." Neglecting those GB, the authors of Ref. 8 found a much larger value, $H_{c1}^c \sim 0.25$ T for a ratio $d/2w \sim 0.1 (N_{eff} \sim 0.9)$. As shown in Fig. 4, this point lies close to the upper solid line, and we can thus reconcile their measurements with ours since Eq. (2) would give a correct H_{c1} value on the order of 0.12 T for this sample. On the contrary, our H_{c1} values are much larger than those recently obtained by Kim *et al.*[7] [still obtained using Eq. (1)]. This discrepancy can *a priori* not be attributed to GB. However, Kim *et al.*[7] deduced H_p from the field at "which deviation from the Meissner shielding occurs" in the global magnetization curve. If this criterion would be perfectly valid for elliptical samples, it can be misleading in the presence of GB. Indeed, since vortices are partially penetrating into the sample through the corners this deviation occurs for fields much lower than H_p for samples with a rectangular cross section.[16] Finally, note that it has been suggested by Golubov *et al.*[17] that H_{c1} can be very sensitive to intraband scattering, and different H_{c1} values could be obtained depending on the sample purity.

Finally, we measured H_p for various angles (θ) between H_a and the c axis. The field measured by the sensors is equal to the perpendicular component of the local induction $B(x)$ and the Hall signal thus rapidly decreases for increasing θ values. However, we were able to determine H_p even for H_a parallel to the ab planes as this plane was making an angle of about 3° with the plane of the probe. The angular dependence of H_p is displayed in the inset of Fig. 4 for sample 6. For a strip with an elliptical cross section H_p would be related to H_{c1} through

$$H_p = \frac{H_{c1}^{ab}}{\sqrt{\left[\frac{\cos(\theta)}{1-N_{eff}}\right]^2 + \left[\frac{\sin(\theta)}{N_{eff}}\right]^2}}, \quad (3)$$

where N_{eff} is the demagnetizing coefficient along the c axis. The solid line in the inset of Fig. 4 is a fit to the data taking $N_{eff}=0.78$ and $\mu_0 H_{c1}^{ab} \sim 0.12$ T. This demagnetization coefficient value is in good agreement with the one calculated by Brandt[11] for a strip with $d/2w \sim 1/3$ (sample 6). In the ab plane, the GB are negligible and as shown, the agreement between the experimental data and Eq. (3) is excellent. However, as θ becomes smaller than $\sim 45°$, H_p becomes progressively larger than the theoretical value of the ellipsoide. This might be interpreted as due to some anisotropy in H_{c1}. However, this deviation is a direct consequence of the GB, which delay the vortex penetration close to the c axis, leading to H_{c1} values larger than those which could be deduced from the ellipsoid formula [Eq. (3)].

In conclusion, we have shown that GB play a dominant role in the origin of irreversibility in high-quality MgB_2 single crystals. Those barriers are superimposed to a small bulk critical current density ($\sim$a few 10^4 A/cm^2 at low temperature and low field). They govern vortex penetration for external fields parallel to the c axis but are negligible for H in the basal planes. We confirm that H_{c1} is isotropic at low temperature being on the order of 0.11 ± 0.01 T. As predicted by the two-band scenario, $\Gamma_{H_{c1}} \ll \Gamma_{H_{c2}}$ at low temperature and those two quantities merge at T_c.

[1] J. Nagamatsu *et al.*, Nature (London) **410**, 63 (2001).
[2] P. Szabó *et al.*, Phys. Rev. Lett. **87**, 137005 (2001); F. Giubileo *et al. ibid.* **87**, 177008 (2001); F. Bouquet *et al.*, Europhys. Lett. **56**, 856 (2001).
[3] L. Lyard *et al.*, Phys. Rev. B **66**, 180502(R) (2002).
[4] S. L. Bud'ko *et al.*, Phys. Rev. B **64**, 180506(R) (2001); M. Angst *et al.*, Phys. Rev. Lett. **88**, 167004 (2002); U. Welp *et al.*, Phys. Rev. B **67**, 012505 (2003).
[5] L. Lyard *et al.*, Phys. Rev. Lett. **92**, 057001 (2004).
[6] V. G. Kogan, Phys. Rev. B **66**, 020509(R) (2002).
[7] H. J. Kim *et al.*, Phys. Rev. B **69**, 184514 (2004).
[8] G. K. Perkins *et al.*, Supercond. Sci. Technol. **15**, 1156 (2002); A. D. Caplin *et al.*, *ibid.* **16**, 176 (2003).
[9] C. P. Bean and J. D. Livingston, Phys. Rev. Lett. **12**, 14 (1964).
[10] E. Zeldov *et al.*, Phys. Rev. Lett. **73**, 1428 (1994).
[11] E. H. Brandt, Phys. Rev. B **59**, 3369 (1999).
[12] E. Zeldov *et al.*, Europhys. Lett. **30**, 367 (1995).
[13] K. H. P. Kim *et al.*, Phys. Rev. B **65**, 100510(R) (2002).
[14] P. F. Sullivan and G. Seidel, Phys. Rev. **173**, 679 (1968).
[15] C. P. Bean, Phys. Rev. Lett. **8**, 250 (1962).
[16] E. H. Brandt, Phys. Rev. B **60**, 11 939 (1999).
[17] A. A. Golubov *et al.*, Phys. Rev. B **66**, 054524 (2002)
[18] V. N. Kopylov *et al.*, Physica C **170**, 291 (1990); M. Konczykowski *et al.*, Phys. Rev. B **43**, R13 707 (1991).